Sizing of an autonomous microgrid considering droop control

Rey, Juan M.; Jiménez-Vargas, Iván; Vergara , Pedro P.; Osma-Pinto, Germán ; Solano, Javier

DOI
10.1016/j.ijepes.2021.107634

Publication date
2022

Document Version
Final published version

Published in
International Journal of Electrical Power & Energy Systems

Electrical Power and Energy Systems 136 (2022) 107634

Contents lists available at ScienceDirect

International Journal of Electrical Power and Energy Systems

journal homepage: www.elsevier.com/locate/ijepes

Sizing of an autonomous microgrid considering droop control☆

Juan M. Rey [a,*], Iván Jiménez-Vargas [a], Pedro P. Vergara [b], Germán Osma-Pinto [a], Javier Solano [a]

[a] Escuela de Ingenierías Eléctrica, Electrónica y de Telecomunicaciones, Universidad Industrial de Santander, Bucaramanga 680002, Colombia
[b] Intelligent Electrical Power Grids Group, Delft University of Technology, Delft, the Netherlands

ARTICLE INFO

Keywords:
Droop control
Microgrids
Renewable energies
Sizing

ABSTRACT

Autonomous microgrids are a suitable solution for off-grid electrification in terms of costs and reliability. The correct sizing of its generation and storage systems ensures efficient utilization of the available energy resources. Generally, many sizing approaches assume optimized energy management strategies that rely on central control architectures. However, these architectures are not always available, especially in limited investment microgrid projects. For this reason, the study of operation scenarios based on decentralized control strategy such as droop control is relevant. Based on this, this paper aims to evaluate the impact of the droop control over the sizing results of a solar/wind/battery/diesel microgrid. For this purpose, a case study of a sizing problem is presented, including the formulation and modelling. Results are presented comparing an hourly optimized energy management scenario with multiple values of the droop control parameters. Simulations results indicate that a competitive total cost can be obtained if the droop parameters are calculated considering the microgrid sizing results. Based on this, a generalizable design methodology for this purpose is presented.

1. Introduction

Autonomous microgrids are recognized as one of the most suitable and cost-effective solutions for off-grid electrification in rural [1,2] or remote applications [3,4]. The main factor influencing this situation is the continuously decreasing costs of renewable energy technologies due to technological advances and increased scales of production. However, due to the intermittent, unpredictable, and seasonal nature of renewable resources, it is highly risky for the reliability of the system to implement autonomous microgrids based exclusively on renewable energy sources. As an alternative, it is recommended to consider the implementation of hybrid systems which integrate renewable sources with multiple storage systems or fuel-based generators as backup systems [5–7]. Hybrid microgrids allow a reliable energy supply and, as it has been widely discussed in the literature, generally its operation is less expensive than single energy source microgrids [8,9].

The microgrid sizing problem is understood as the design and quantification of the generation and storage systems. For the reasons stated above, the formulation and solution of the microgrid sizing become fundamental to ensure efficient utilization of the generation sources in hybrid systems [10]. The suitable sizing of the microgrid reduce the risk of oversize (which could lead to high costs) or undersize (which can risk the power supply reliability) the elements of the system and avoids its undesired consequences [11].

As shown in [12], several methodologies have been presented to address the sizing problem of hybrid microgrids in different applications and scenarios. One of the most commonly analyzed configurations for the generation and storage systems corresponds to a microgrid composed of solar/wind/battery/diesel generators [13,14]. When a proper sizing is calculated, this type of microgrid allows a good balance between renewable and fuel-based power generation, and thus, between implementation costs and power supply reliability [15].

Several works have explored different sizing approaches of this microgrid configuration considering complementary design criteria such as techno-economic feasibility [16–18], life-cycle costs and emissions [19,20], human development indices [21], levelized costs of energy [22–24] or environmental impacts indicators [25], formulating and modeling the mathematical problem or using specialized software for this purpose, as HOMER [26–28]. Also, other works are focused on testing the performance of different optimization techniques such as teaching-learning optimization [29], diving rectangles algorithm [30], particle swarm optimization [31,32], self-adaptive differential evolution

☆ This work was supported by Universidad Industrial de Santander and Minciencias, with project "Programa de Investigación en Tecnologías Emergentes para Microredes Eléctricas Inteligentes con Alta Penetración de Energias Renovables", contract No. 80740-542-2020.

* Corresponding author.
E-mail address: juanmrey@uis.edu.co (J.M. Rey).

https://doi.org/10.1016/j.ijepes.2021.107634
Received 25 February 2021; Received in revised form 18 June 2021; Accepted 17 September 2021
Available online 5 October 2021

[29], grasshopper algorithm [33], clonal selection algorithm [34], social spider algorithm [35], elephant herd algorithm [36] and other bio-inspired optimization approaches [37–39] on the solar/wind/battery/diesel generators microgrids sizing solution.

Regarding microgrids operation, hierarchical control has become the standard approach to control and coordinate the critical functioning variables [40,41]. In the hierarchical approach, the control objectives are managed in layers according to their dynamics of operation [42,43]. The most common hierarchical architecture considers a three-layer scheme [44], in which the superior layers control the power quality and energy dispatch. In contrast, the primary layer regulates the local frequencies of the distributed generators until a global frequency is reached. The primary layer objectives can be achieved using different control strategies, with droop control being one of the most remarkable [45]. The action of the droop control produces a linear deviation that relates the frequency and the active power. Thus, once a steady-state global frequency is reached, a power-sharing between the distributed generators is achieved.

Despite the common use of the droop control due to its implementation simplicity, many sizing approaches fail to consider its operation in the problem formulation. The main reason for this is that it is assumed that a centralized architecture based on a microgrid central controller (MGCC) is implemented. MGCC periodically sends dispatch signals to the controllable distributed generators in order to ensure optimal energy management. However, the availability of an MGCC is not always ensuring, especially in limited investment projects. Taking into account that many microgrids, especially those that operate in rural and remote areas, could operate using strategies that are based only on local control techniques, it is relevant to evaluate its impact on the use of energy resources [46].

Some of the key works that have studied the impact of droop control on autonomous microgrids are the following. Regarding the operation, in [47] a sitting and operation method to set the droop control parameters of distributed generators is presented. These parameters are defined solving an optimization problem to reduce fuel cost and improve voltage profile and stability. In [48] a formulation for reconfiguration of autonomous droop-based microgrids is presented. In [49,50] are proposed optimal allocation and volt-var dispatch strategies for achieving reactive power-sharing, reduction of line losses and conservation voltage reduction in droop-based autonomous microgrids. Also, an allocation of active and reactive power among dispatchable generators in droop controlled microgrids is proposed in [51]. This strategy considers economic, environmental and operational control objectives.

Regarding the sizing, in [52] the energy storage systems of a standalone microgrid that works based on droop control are designed to support the regulation and enhance stability. Also, in [53] a sizing of the battery energy storage is performed implementing a frequency regulation function. In [54] the sizing of the generation and storage systems of a droop-based microgrid is studied in the context of expansion planning.

To date, for the authors' best knowledge, there are no reported works that explicitly study the impact of considering droop control on cost and reliability indicators of generation and storage units sizing design of autonomous microgrids. Thus, the main contributions of this work are the following:

- An evaluation of the impact of considering droop control as operation technique on sizing results is presented. For this purpose, a case study of a solar/wind/battery/diesel microgrid sizing is modelled and simulated. The results are compared with an ideal centralized hourly optimized energy management scenario to identify how the droop parameters can be appropriately defined from the microgrid sizing approach.
- A generalizable design methodology to calculate droop parameters considering the microgrid sizing results is presented.

The rest of the paper is organized as follows: Section 2 describes the system and modelling. Section 3 presents the power dispatch scenarios, including an hourly optimized energy management and the droop control. In Section 4, information about the case of study is described. Sizing design criteria are presented in Section 5. In Section 6, simulation results are presented and a generalizable design methodology is discussed. Finally, general conclusions are drawn in Section 7.

2. System description and modelling

The system evaluated in this work is an isolated microgrid composed of solar, wind and diesel-based generation sources. The energy storage is performed using batteries. For simplicity, the topology of the grid is assumed as a single AC bus where loads are grouped and connected. Fig. 1 presents a general scheme of the considered system. In this section, the equations that model the power generation systems, the storage system and the energy management strategy are presented.

2.1. PV panels

The model used for the PV panels considers the solar irradiation I and the ambient temperature T_a as input variables [55–57]. First, the cell temperatue T_c is calculated as follows

$$T_c(t) = T_a(t) + I(t)\left(\frac{\mathrm{NOCT} - 20}{0.8}\right) \tag{1}$$

where NOCT is the nominal operating temperature of the PV cells. Using this value, the output power of a single PV panel $P_{PV\mathrm{unit}}$ is calculated as follows

$$P_{PV\mathrm{unit}}(t) = Y_d \eta_{PV} A_{PV} I(t)\left(1 - \frac{K_p}{100}(T_c(t) - 25)\right) \tag{2}$$

where Y_d is a derating factor due to dust accumulation, η_{PV} is the conversion efficiency of the PV panel, A_{PV} is the superficial area of the PV panel and K_p is a power temperature coefficient.

In order to obtain the total power generated by a set of N_{PV} panels, (2) can be replied as

$$P_{PV}(t) = N_{PV} P_{PV\mathrm{unit}}(t). \tag{3}$$

2.2. Wind turbines

The model considered for the wind turbines is based on the following

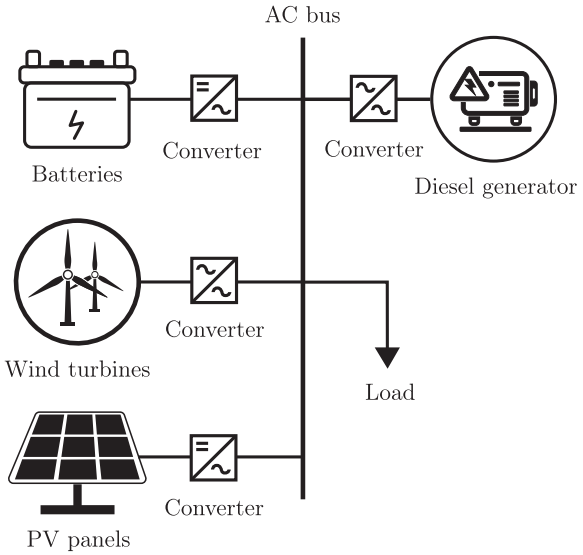

Fig. 1. General scheme of the microgrid considered in the study case.

curve equation [58,59]

$$P_{WT\text{unit}}(t) = \begin{cases} 0 & , V(t) < V_{\text{cut-in}} \\ \left(\dfrac{P_{WT_r}(V^3 - V^3_{\text{cut-in}})}{V^3_{\text{rated}} - V^3_{\text{cut-in}}}\right) & , V_{\text{cut-in}} \leqslant V(t) < V_{\text{rated}} \\ P_{WT_r} & , V_{\text{rated}} \leqslant V(t) < V_{\text{cut-out}} \\ 0 & , V_{\text{cut-out}} \leqslant V(t). \end{cases} \quad (4)$$

where $P_{WT\text{unit}}$ is the output power of a single wind turbine, P_{WT_r} is the rated power of the turbine, V is the wind speed and $V_{\text{cut-in}}$, V_{rated} and $V_{\text{cut-out}}$ are the cut-in, nominal, and cut-out speed of the wind turbine, respectively.

In order to obtain the total power generated by a set of N_{WT} wind turbines, (4) can be replied as

$$P_{WT}(t) = N_{WT} P_{WT\text{unit}}(t). \quad (5)$$

2.3. Diesel generator

For the diesel generator model, operation bounds are considered to avoid overloads or lightly loaded scenarios [60]. These limits are defined based on the nominal power of the diesel generation unit P_{D_r}. Thus, the power of the diesel is defined as

$$P_{D\text{min}} \leqslant P_{D\text{unit}}(t) \leqslant P_{D\text{max}}. \quad (6)$$

For a set of N_D diesel generators, the operation limits in (6) are adapted as

$$N_D P_{D\text{min}} \leqslant P_D(t) \leqslant N_D P_{D\text{max}}. \quad (7)$$

2.4. Batteries

The batteries modeling is based on the power of charge P_{BC} and discharge P_{BD}, which affect the state-of-charge (SOC) [61]. Thus, SOC for t is calculated for a set of N_B batteries according to the injected/extracted powers and the SOC of the last time interval as follows

$$\text{SOC}(t) = \text{SOC}(t - \Delta t) + P_{BC}\frac{\eta_{BC}\Delta t}{N_B Q_{B\text{unit}}} - P_{BD}\frac{\Delta t}{\eta_{BD} N_B Q_{B\text{unit}}} \quad (8)$$

where $Q_{B\text{unit}}$ is the battery capacity of a single unit, η_{BC} is the battery charging efficiency, η_{BD} is the battery discharging efficiency and Δt is the time interval of the power flow analysis. Notice that due to physical restrictions, only one of the last two terms of (8) is used at a time according to the state of the battery (charge or discharge). Maximum charge and discharge rates for a single unit, $P_{C\text{runit}}$ and $P_{D\text{runit}}$, respectively, must be considered, thus

$$0 < P_{BC} \leqslant N_B P_{C\text{runit}} \quad (9)$$

$$0 < P_{BD} \leqslant N_B P_{D\text{runit}}. \quad (10)$$

Also, for the proper operation of the batteries, maximum and minimum values of SOC must be set as operation constraints (SOC_{max} and SOC_{min}, respectively) as

$$\text{SOC}_{\text{min}} \leqslant \text{SOC}(t) \leqslant \text{SOC}_{\text{max}}. \quad (11)$$

2.5. Microgrid operation modes

The microgrid can operate in four operation modes according to the load/supply power balances. These modes are indicated in the flowchart of Fig. 2. Defining the power P_{dif} as the difference between the power demanded by the load P_{load} and the power generated by the renewable sources $P_{PV} + P_{WT}$ (non-dispatchable power sources)

$$P_{\text{dif}}(t) = P_{\text{load}}(t) - P_{PV}(t) - P_{WT}(t). \quad (12)$$

it is possible to indicate that an excess of renewable power generation is presented when $P_{\text{dif}} \leqslant 0$. The power surplus can be fully or partially stored in the batteries according to the maximum capacity of charge $P_{B\text{max}}$. A curtailment strategy is applied on the controllers of the renewable source to avoid overcharge.

On the contrary, a value of $P_{\text{dif}} \geqslant 0$ in (12) indicates insufficient renewable power generation to supply the demanded load. Then, the storage system and the diesel generators must attend the load as long as

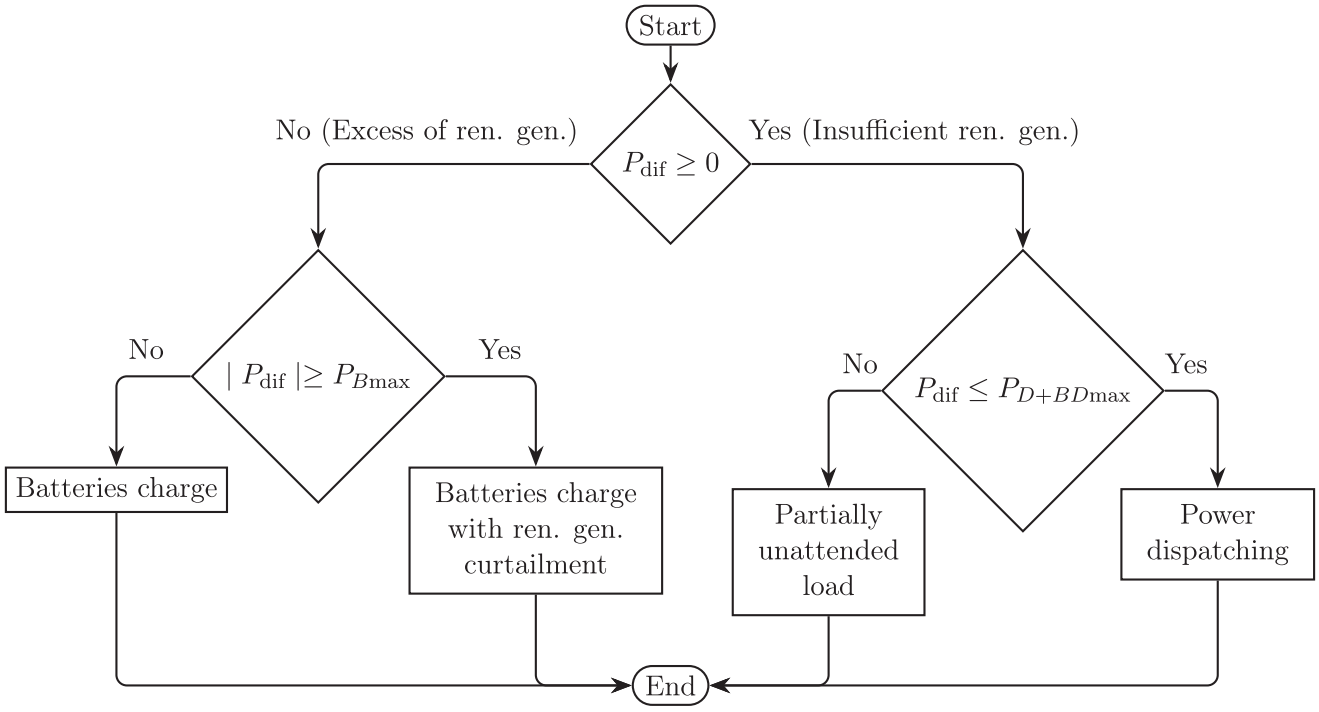

Fig. 2. Flowchart of the microgrid operation modes.

the maximum capacity of these dispatchable sources $P_{D+BD\max}$ allows it. If it is not possible, the load will be partially unattended.

When the load can be attended by the storage system and the diesel generators, the power references of these sources must be defined by the power dispatch. In this paper, two possible strategies of power dispatch are evaluated: an hourly optimized method, which will be used as a benchmark, and the droop control, whose performance integrated with the sizing design will be the focus of the analysis. These power dispatch techniques are presented in the following subsection.

3. Power dispatching

According to the power balance flowchart presented in Fig. 2, the power dispatching is carried out when the renewable power generation is not enough to satisfy the demanded load. Thus, the controllable sources (i.e., the storage system and the diesel generators) must operate delivering the required power. As this work aims to analyze the impact of considering the droop control operation in the sizing formulation, two scenarios are proposed: a first scenario in which an hourly optimized energy management scenario is considered (which will be used as a benchmark in the discussion and analysis of results) and a second scenario with the controllable sources operating with droop control.

3.1. Hourly optimized energy management

In this scenario, a minimization problem is formulated each hour as follows

$$\min_{P_D, P_{DB}} \{f_D + f_{DB}\} \tag{13}$$

where f_D represents the cost function of the diesel generation and f_{DB} is a function that penalizes the discharge of batteries. This minimization is solved subject to the operational constraints in (7)–(11). More details about these cost functions are given in Section 4.2.

3.2. Droop control

The droop control is based on mimicking the behaviour of synchronous generators using the grid-forming sources of the microgrid for this purpose. The angular frequency ω is calculated as follows

$$\omega = \omega_0 - mP \tag{14}$$

where ω_0 is the reference angular frequency, m is the droop gain and P is the supplied active power.

As a global steady-state frequency is reached, a power-sharing relation is obtained. Thus, if the microgrid has n sources working with the control law in (14), the power-sharing will be defined by

$$m_1 P_1 = m_2 P_2 = \ldots = m_n P_n. \tag{15}$$

Notice that the operation of the droop control set a power-sharing between the supplied active powers according to the values of the gains implemented in each source. Thus, the operation is restricted by this relation, and the power generators do not necessarily operate in an optimal point [62]. As previously discussed, although the droop control approach is not an optimal dispatch strategy in terms of energy resources use, this is a realistic operating scenario in microgrids in which an MGCC is not implemented, and the operation of the grid relies on the local controllers of the power generators units.

4. Case of study

As case study, a microgrid that follows the scheme and modelling presented in Section 2 is considered. The values of the implemented parameters are listed in Table 1, where P_{PV_r} is the rated power of the PV panels, $P_{Cr\text{unit}}$ and $P_{Dr\text{unit}}$ are the maximum charge and discharge rates for a single battery, respectively. The rest of the parameters were previously described.

Table 1
Implemented parameters.

Symbol	Quantity	Units	Symbol	Quantity	Units
P_{PV_r}	0.34	kW	$Q_{B\text{unit}}$	9.8	kWh
NOCT	45	$^\circ C$	$P_{Cr\text{unit}}$	3	kW
Y_d	0.9	–	$P_{Dr\text{unit}}$	5	kW
η_{PV}	0.175	–	$SOC_{\min}$	0.4	–
A_{PV}	1.944	m^2	$SOC_{\max}$	1	–
K_p	−0.35	$\%/^\circ C$	SOC_0	0.5	–
P_{WT_r}	10	kW	N_c	2000	cycles
$V_{\text{cut}-\text{in}}$	3	m/s	P_{D_r}	5	kW
V_{rated}	10	m/s	C_{diesel}	1	USD/L
$V_{\text{cut}-\text{out}}$	20	m/s			

4.1. Meteorological and load consumption data

Meteorological information is used in sizing problems as input data. In this study, the input of the power generation modelling corresponds to the solar irradiation I, the ambient temperature T_a for the PV model, and wind speed V. As case study, a location at latitude 12.154 longitude −72.063 on the north of Guajira region in Colombia was considered. The meteorological data for one year was obtained from EU Science Hub database. Three days in a row of the analyzed time interval were randomly chosen to be shown in Fig. 3.

For the load consumption, a standard normalized profile was implemented (see Fig. 4), which is used assuming a nominal demanded power of 20 [kW]. The annual load profile was calculated considering a randomness factor of ± 15% to introduce a variability.

4.2. Cost functions

The cost functions consist of two components: an implementation cost (CAPEX) which includes the installation and replacements costs and quantifies the salvage costs, and an operation cost (OPEX) which includes operation and maintenance (O&M) and fuel costs. For the CAPEX component, the value of each unit is calculated using the rated powers and the factors presented in Table 2. For OPEX component, the functions are modeled considering the following diesel consumption equation [33,63]

$$f_D(P_D) = \beta_D P_D + \gamma_D \tag{16}$$

where β_D and γ_D are constants that are calculated as follows

$$\beta_D = 0.246\ C_{\text{diesel}} \tag{17}$$

$$\gamma_D = 0.08415\ C_{\text{diesel}}\ P_{D_r}\ N_D. \tag{18}$$

where C_{diesel} is the cost of the fuel, P_{D_r} the rated capacity of the generating unit and N_D is the total number of diesel generators.

For the batteries, the cost of operation (degradation function) is modeled penalizing the discharge power as [64]

$$f_{BD}(P_{BD}) = \alpha_{BD} P_{BD}^2 \tag{19}$$

where α_{BD} is a constant calculated considering the cost C_B, the life time in cycles N_c, the depth of discharge DoD, and the capacity of the battery $Q_{B\text{unit}}$, as follows

$$\rho_0 = \frac{C_B}{2\ N_c\ \text{DoD}\ Q_{B\text{unit}}} \tag{20}$$

$$\alpha_{BD} = \frac{\rho_0}{0.6\ P_{Dr\text{unit}}\ N_B}. \tag{21}$$

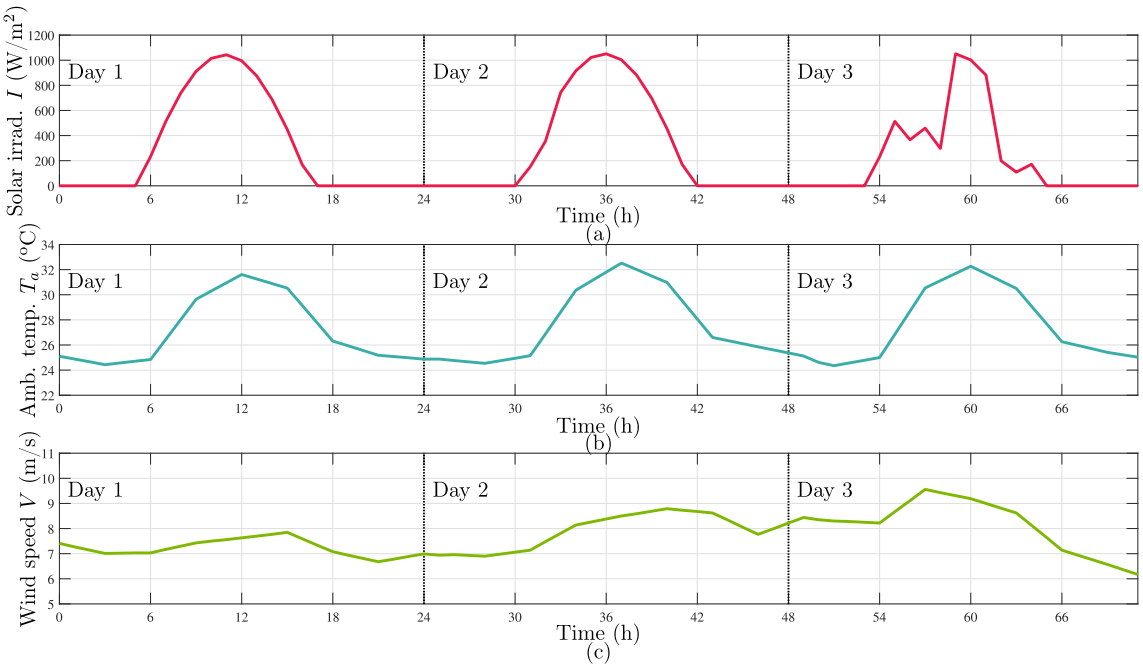

Fig. 3. Solar irradiation I, ambient temperature T_a and wind speed V for three days of the case study.

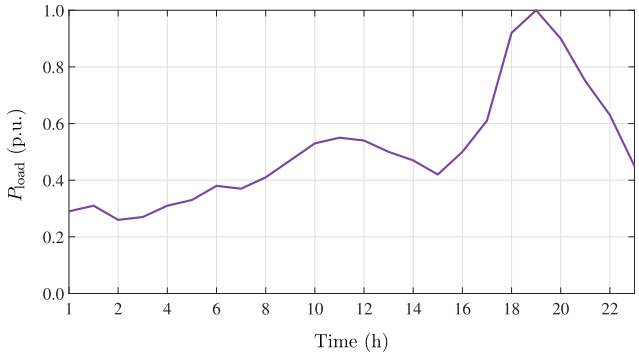

Fig. 4. Standard normalized profile considered for the load consumption.

Table 2
CAPEX and O&M factors of the cost functions.

Symbol	Quantity	Units	Symbol	Quantity	Units
$C_{PVcapex}$	3200	USD/kW	$C_{PVO\&M}$	30	USD/kW-YEAR
$C_{WTcapex}$	4000	USD/kW	$C_{WTO\&M}$	45	USD/kW-YEAR
C_{Bcapex}	1060	USD/kW	$C_{BO\&M}$	15	USD/kW-YEAR
C_{Dcapex}	600	USD/kW	$C_{DO\&M}$	0.034	USD/kW-HOUR

Cost functions in (16) and (19) are applied in the hourly optimal dispatch equation described in (13). An additional O&M terms to model the annual maintenance costs are considering using the rated powers and the factors presented in Table 2.

5. Sizing design criteria

In general, solving the sizing problem of a hybrid system requires satisfying a compromise between power supply reliability and cost. In order to quantify the reliability of the microgrid, different approaches have been presented in the literature. In this paper, two of the most commonly used reliability indicators are considered: LPSP and LOLH [11,10,65].

- Loss of Power Supply Probability (*LPSP*): This design criterion quantifies the probability to have unsupplied demand during the time of analysis. For this purpose, the loss of power supply *LPS* is calculated, which corresponds to the hourly unsupplied load (occurs in the operation mode in which neither generation nor storage has the capacity to fully satisfy the load, as explained in Section 2.5). Then, *LPSP* is obtained from the ratio between the total sum of *LPS* and the total demanded load P_{load}, as follows

$$LPSP = \frac{\sum LPS}{\sum P_{load}} 100\% \tag{22}$$

- Loss of Load Hours (*LOLH*): This design criterion quantifies the percentage of hours of the time of analysis in which the load is partially unattended. For this, *HLPS* is calculated, being the total of hours in which *LPS* has a non-zero value. Then, *LOLH* is obtained from the ratio between *HLPS* and the total hours of analysis *N*. It can be expressed as

$$LOLH = \frac{HLPS}{N} 100\% \tag{23}$$

Maximum values for these criteria are defined to discard unfeasible sizing solutions. Any sizing solution with reliability criteria values lower than these values is considered viable or feasible, and from this group is selected the one with lower total cost as the best solution. This procedure is explained in detail in the next section.

6. Results and discussion

This section presents selected simulation results to analyze the impact of considering the droop control operation in the sizing problem of an autonomous microgrid. Based on these results, a design methodology to calculate droop parameters is presented.

The solution of the sizing scenarios follows a common procedure: first, a wide enough search space is defined based on the load peak (nominal demanded power). It is worth noting that a definition of design

rules or a proper optimization solver method could significantly reduce the total computation time. However, this procedure was not detailed in this work since it is not relevant to the proposed discussion. Then, an hourly microgrid power balance is solved considering generated and consumed powers, storage capacity and the power dispatch strategies, i.e., optimized EM or droop control. Based on this, the reliability criteria are calculated. A maximum value of 2.5% was considered for LOLH and LPSP indicators. Finally, the best solution is determined by selecting the lower total cost (i.e., CAPEX and OPEX) of the viable solutions.

6.1. Sizing considering hourly optimized energy management strategy

First, the sizing problem was solved considering the hourly optimized EM (described in Section 3.1). Notice that the interest of this work is to evaluate the impact that the droop control has over the sizing results, for this reason, these results are used as a benchmark in the analysis and discussion. Fig. 5 presents all the obtained solutions in a LPSP vs COST plot. A total of 113117 solutions are considered viable according to the reliability indicators.

In order to discard infeasible solutions, a pareto front is plotted in Fig. 6. The cost components and reliability indicators of the hourly optimized EM solution are also presented. This optimal solution is composed by the following configuration: $N_D = 2$ [units], $N_{WT} = 3$ [units], $N_{PV} = 66$ [units] and $N_B = 6$ [units]. The reliability performance of this configuration was evaluated in the following subsection for different values of droop control parameters.

6.2. Evaluation of the impact of droop control operation over sizing results

In this subsection, an evaluation of the impact of considering droop control as operation technique over the sizing results is performed. From this approach, a methodology to design the droop control parameter is proposed. As a starting point, notice that, according to (15), the values of the gains m_i have a direct impact on the power-sharing between supplied active powers, and thus, over the operation of the microgrid. As discussed in Section 3, although this operating restriction may not be an optimal operating point, it is how microgrids based on static control droop control are expected to operate. For simplicity, in this study, each type of generation/storage system was considered as a set, and thus, it is controlled setting a single droop control parameter. Then, (15) can be rewritten as

$$m_D P_D = m_{BD} P_{BD}. \tag{24}$$

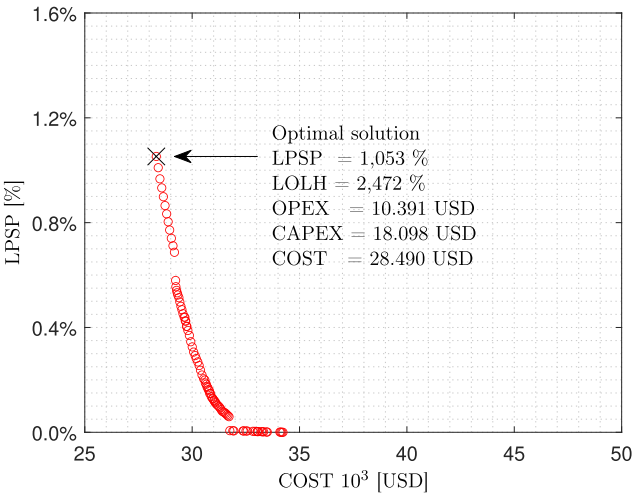

Fig. 6. Pareto front of sizing solutions considering the hourly optimized EM.

Realize that (24) indicates that the design of the gains m_D and m_{BD} is key to determine the proportion of the supplied active powers. Lets define X_m as the ratio

$$X_m = \frac{m_{BD}}{m_D} = \frac{P_D}{P_{BD}}. \tag{25}$$

Some works suggest designing the ratio X_m as a proportion of the nominal powers of the dispatched sources [66]. However, in the sizing problem these nominal powers are not known in advance (in fact, they are obtained by solving the sizing problem). So that, to analyze the impact of varying the droop ratio X_m over the sizing results, multiple values of this variable were tested by solving several sizing scenarios.

As a first case, the configuration obtained from the sizing solution considering the hourly optimized EM (i.e., $N_D = 2$ [units], $N_{WT} = 3$ [units], $N_{PV} = 66$ [units] and $N_B = 6$ [units]) was evaluated for selected values of X_m. The reliability indicators are presented in Fig. 7. Two remarkable aspects can be concluded from these results: on the one hand, it is observed that all values of the ratio X_m present non-feasible solutions (i.e., LOLH and LPSP above 2.5%.). Indeed, in some cases, reliability indicators present values above 10%, which correspond to unfeasible solutions with a poor reliability performance. On the other hand, the simulations results show that the impact over the reliability indicators does not produce significant changes when $X_m \geqslant 25$, reaching

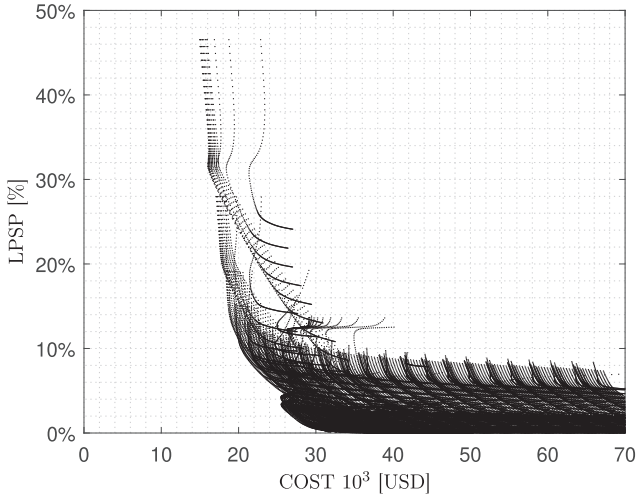

Fig. 5. LPSP vs COST of all sizing solutions considering the hourly optimized EM.

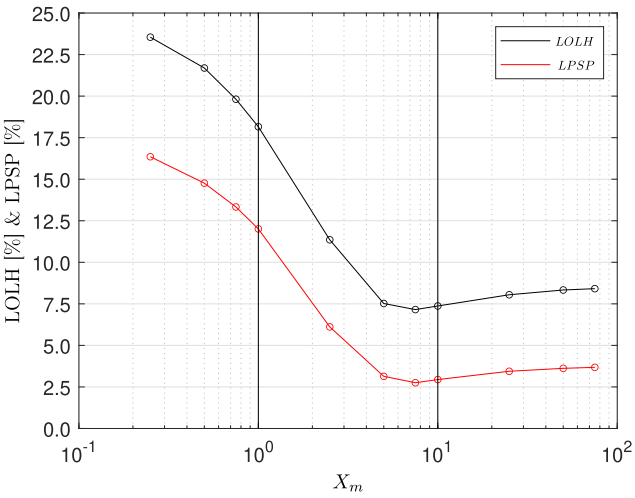

Fig. 7. Best microgrid configuration with the hourly optimized EM evaluated with selected values of ratio X_m.

almost constant values. The reason is that, for this interval, the ratio between the delivered powers P_D and P_{BD} makes the power contribution of the batteries almost negligible.

This first analysis shows that given a specific microgrid size configuration, droop control has a poor performance in terms of reliability compared with the centralized hourly optimized EM. However, as will be discussed later, this can be overcome if the design of the variable X_m is considered in the sizing formulation.

Next, the sizing problem was solved for selected values of X_m. Unlike the previous results, in this case, a configuration was not fixed in advance, but the sizing problem was solved (calculating the best sizing solution) for each of the values of the set $X_m = [0.25, 0.5, 0.75, 1, 2.5, 5, 7.5, 10, 25, 50, 75]$. In all the simulations, the same search space was considered. The main findings are discussed and illustrated below. The sizing results considering the centralized hourly optimized EM are presented (using the convention OPT) as a benchmark.

- **Viable Solutions:** For each tested value of X_m, different amounts of viable solutions were obtained (for $X_m = 0.25$ no feasible solution was found). The results are presented in Fig. 8. It can be appreciated that the number of viable solutions increases when the value of the ratio X_m is greater. It is worth noting that this trend does not necessarily mean that less expensive configurations are obtained in largest values of X_m, as will be discussed below.
- **Reliability Indicators:** The reliability indicators of the best sizing solution for each value of X_m are presented in Fig. 9. Notice that, in general, the dominant reliability indicator is LOLH, which means that this is the indicator that is closest to the defined threshold (2.5%). For this reason, it is the most critical reliability criterion to determine if a configuration is viable or not.
- **Costs Components:** The cost components of the best sizing solution for each value of X_m are presented in Fig. 10. CAPEX and OPEX were highlighted using different colours. This figure shows that the sizing result of the hourly optimized EM corresponds to the cheapest solution. This is because the operation of the hourly optimized EM strategy guarantees the best OPEX performance. However, it is also possible to observe that some values of X_m present sizing solutions with highly competitive costs solution compared to this benchmark. Particularly, the total costs of the best configurations with $X_m = 5$, 7.5, 10 and 25, are more expensive for less than 10% compared with the hourly optimized EM solution.

The obtained results indicate that a more detailed exploration of the values of X_m in the range $5 \leqslant X_m \leqslant 25$ is convenient in order to identify the ratio with the best sizing results. For this analysis, a step of 0.25 in the ratio was considered. The total costs of the best sizing solution for each value of X_m in this range are presented in Fig. 11.

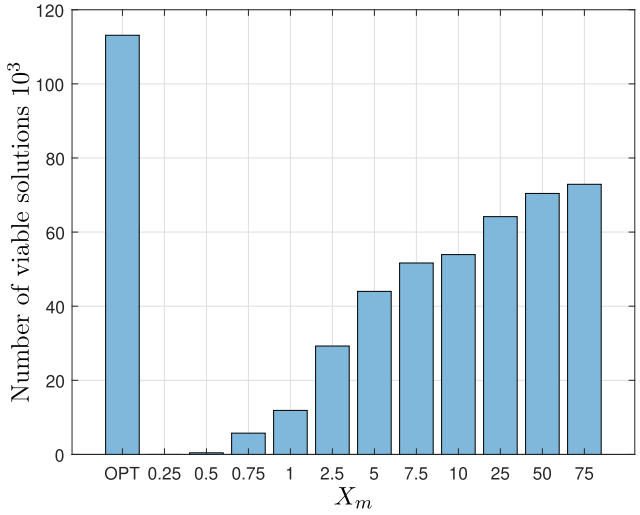

Fig. 8. Number of viable solutions for the hourly optimized EM and different values of X_m.

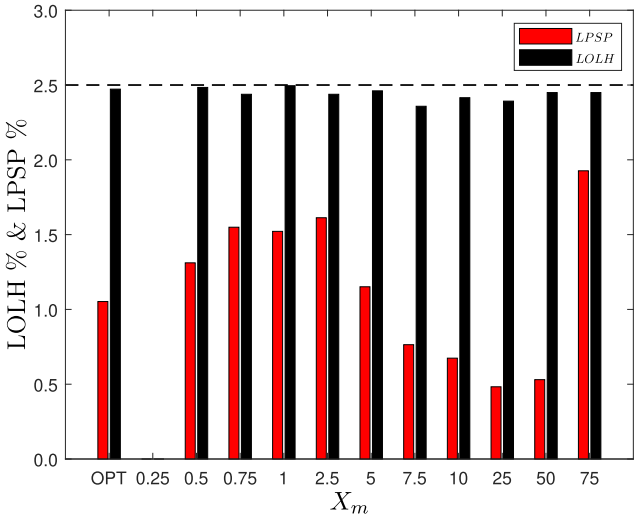

Fig. 9. Reliability indicators of the best sizing solutions for the hourly optimized EM and different values of X_m.

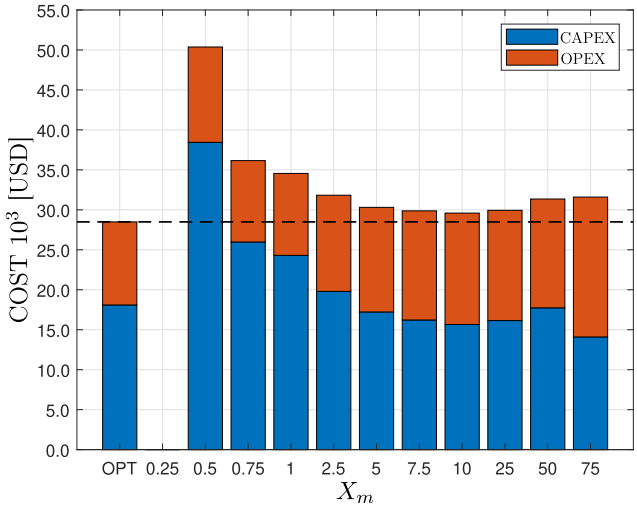

Fig. 10. Cost of the best sizing solutions for the hourly optimized EM and different values of X_m.

These results show that the cheapest sizing configuration is obtained using $X_m = 21.25$. The total cost obtained is only 2.36% more expensive than the solution considering the hourly optimized EM, which indicates that a proper droop parameters design could lead to a suitable microgrid operation in terms of cost and reliability without depending on a dispatch strategy that relies on the implementation of MGCC. This solution is composed by the following configuration: $N_D = 3$ [units], $N_{WT} = 3$ [units], $N_{PV} = 47$ [units] and $N_B = 8$ [units]. Table 3 presents the configuration of the best sizing solution of the main values of X_m tested. In this table, Δ_{COST} is the percentage difference of the total cost of the configuration with respect to the hourly optimized EM solution. A discussion of the operating performance of the selected sizing configuration is presented in the following subsection.

6.3. Operation of the selected sizing solution for droop control

The selection of a ratio X_m sets an operating power-sharing relation between the dispatchable sources of the selected sizing solution. When

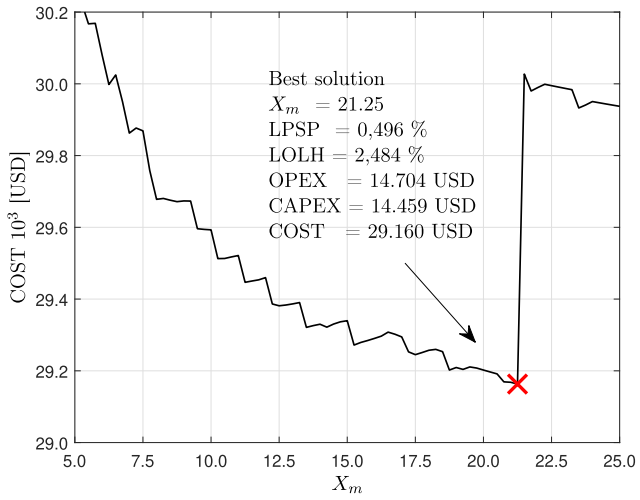

Fig. 11. Cost of the best sizing solutions for a selected range of values of X_m.

simulating the hourly generation-load power balance, it can be observed that due to the selection of X_m has been made from a sizing design approach where operational criteria are considered (reliability criteria described in Section 5), overstress of the sources because of a permanent operation near their operating limits is prevented.

To illustrate this, in Fig. 12 is presented the hourly generation-load powers of the days in which the diesel generation and batteries operate delivering their greatest powers. In this figure can be seen that even in these selected days, the dispatchable sources are only delivering maximum powers at some singular operating situations, for instance, when the wind resource is particularly low during a peak load consumption. According to the simulations results, diesel generators work at more than 95% of their nominal capacity in less than 4.5% of the hours of analysis, which is considered an acceptable operation that does not compromise the lifespan of the equipment and the reliability of the microgrid.

6.4. Design of droop parameters considering microgrid sizing

The case study presented in the previous subsections showed the impact that the operation based on the droop control can have over the microgrid sizing. The results show that a competitive cost can be obtained if the droop parameters are designed considering the sizing formulation. Intending to generalize this design approach, Fig. 13 presents the scheme that summarizes the suggested methodology to calculate the droop parameters considering the sizing results.

The design methodology consists of solving the microgrid sizing problem for a set of values of the droop ratio X_m. The values of this set can be defined by setting a fixed step or, as was presented in the case study, evaluating for selected values to analyze the costs behaviour, and then exploring the results for a specific range of values of X_m. Obtaining the best sizing solutions for each value (this implies that, as they are viable solutions, the defined reliability thresholds are guaranteed) lead to the selection of the best X_m in terms of total costs.

It is worth noting that the proposed design methodology allows obtaining a value for X_m, which corresponds to a ratio between the droop control parameters (see (25)). This value is related to a desired power-sharing behaviour, and thus, there are multiple values of m_{BD} and m_D with which this ratio X_m can be obtained. For this reason, before setting droop parameters, a stability analysis must be performed. This last step is necessary to guarantee proper stability and dynamic characteristics. In the specialized literature on microgrids, there are several works focused on describing the stability analyses of droop control. Usually, these are based on design rules that consider the maximum allowable frequency deviations or stability rules based on small-signal analysis [67,68].

7. Conclusions

This work aims to analyze the impact of droop control over the sizing results of a solar/wind/battery/diesel microgrid. For this purpose, a case study was modelled and simulated as a numerical example. As a benchmark, an hourly optimized EM scenario was solved. The main conclusions are the following:

- The droop control operation has a major impact on the microgrid sizing. Thus, the best sizing solution for an hourly optimized EM

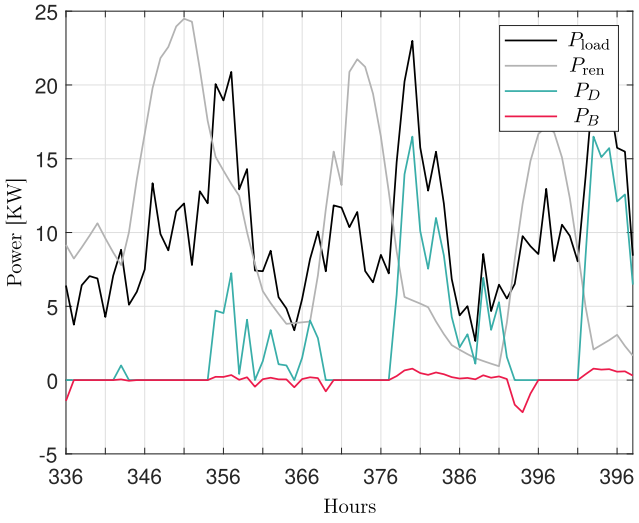

Fig. 12. Generation-load powers for selected days.

Table 3
Best sizing solutions for the optimal dispatch and different values of X_m.

X_m	OPT	0.25	0.5	0.75	1	2.5	5	7.5	10	**21.25**	25	50	75
N_D [units]	2	–	2	2	2	3	3	3	3	**3**	3	3	4
N_{WT} [units]	3	–	9	3	3	3	3	3	3	**3**	4	5	3
N_{PV} [units]	66	–	148	113	104	80	63	57	54	**47**	45	40	26
N_B [units]	6	–	15	15	14	9	9	9	9	**8**	8	8	8
LPSP	1,053%	–	1,311%	1,550%	1,522%	1,613%	1,151%	0,764%	0,674%	**0,496%**	0,483%	0,530%	1,926%
LOLH	2,472%	–	2.484%	2,438%	2,495%	2,438%	2,461%	2,358%	2,415%	**2,484%**	2,392%	2,450%	2,450%
OPEX [USD]	10.391	–	11.931	10.177	10.251	12.032	13.081	13.648	13.935	**14.704**	13.789	13.613	17.499
CAPEX [USD]	18.098	–	38.439	25.978	24.303	19.795	17.226	16.221	15.658	**14.459**	16.148	17.739	14.097
COST [USD]	28.490	–	50.369	36.155	34.554	31.827	30.308	29.869	29.593	**29.160**	29.937	31.352	31.596
Δ_{COST}	0%	–	76.80%	26.90%	21.28%	11.71%	6.38%	4.84%	3.87%	**2.35%**	5.08%	10.04%	10.90%

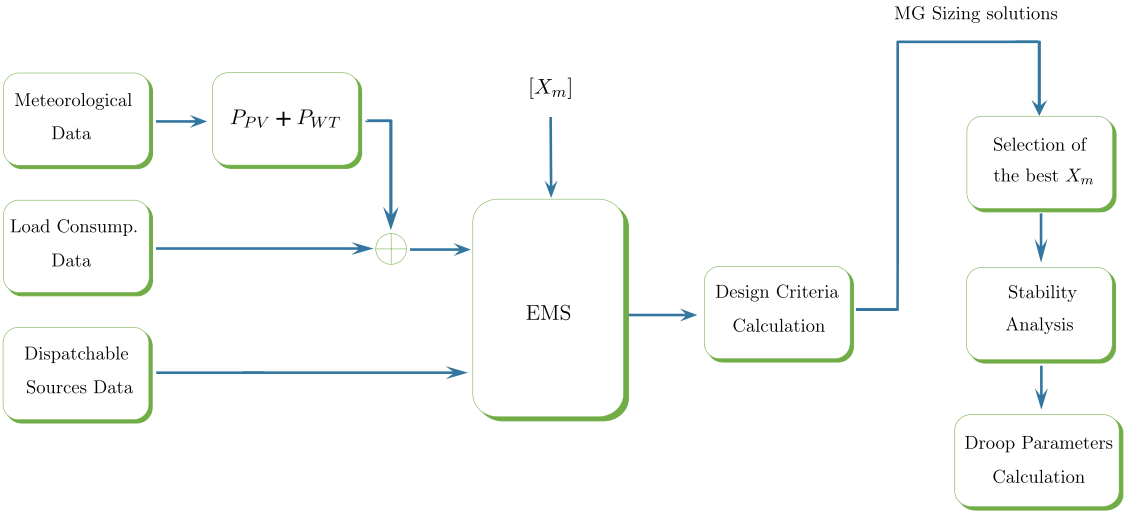

Fig. 13. Design methodology to calculate droop parameters considering MG sizing.

scenario does not necessarily guarantee good performance for droop control.

- The obtained results indicate that a highly competitive sizing solution in terms of total costs can be obtained if the droop control parameters are calculated using a design methodology that integrates the sizing approach. In the case study presented, this difference is less than 2.4%, which is an excellent result considering droop control does not require a centralized controller.
- A generalizable design methodology to calculate droop parameters was presented. Unlike other approaches, this proposal considers the microgrid sizing results as starting point to select a ratio X_m that guarantees a competitive total cost for microgrids that operate without centralized control strategies.

Future research will be focused on analyzing the impact of adaptive droop control strategies in different microgrids configurations and operating scenarios.

Declaration of Competing Interest

The authors declare that they have no known competing financial interests or personal relationships that could have appeared to influence the work reported in this paper.

References

[1] Ubilla K, Jiménez-Estévez GA, Hernández R, Reyes-Chamorro L, Hernández Irigoyen C, Severino B, et al. Smart microgrids as a solution for rural electrification: Ensuring long-term sustainability through cadastre and business models. IEEE Trans Sustain Energy 2014;5:1310–8.
[2] Kumar A, Singh AR, Deng Y, He X, Kumar P, Bansal RC. A novel methodological framework for the design of sustainable rural microgrid for developing nations. IEEE Access 2018;6:24925–51.
[3] Parida A, Choudhury S, Chatterjee D. Microgrid based hybrid energy co-operative for grid-isolated remote rural village power supply for east coast zone of India. IEEE Trans Sustain Energy 2018;9:1375–83.
[4] Barbaro M, Castro R. Design optimisation for a hybrid renewable microgrid: Application to the case of faial island, azores archipelago. Renew Energy 2020;151:434–45.
[5] Mahmood H, Michaelson D, Jiang J. Strategies for independent deployment and autonomous control of PV and battery units in islanded microgrids. IEEE J Emerg Sel Top Power Electron 2015;3:742–55.
[6] Sachs J, Sawodny O. A two-stage model predictive control strategy for economic diesel-PV-battery island microgrid operation in rural areas. IEEE Trans Sustain Energy 2016;7:903–13.
[7] Abo-Elyousr FK, Elnozahy A. Bi-objective economic feasibility of hybrid micro-grid systems with multiple fuel options for islanded areas in egypt. Renew Energy 2018;128:37–56.
[8] Rey JM, Vergara PP, Solano J, Ordóñez G. Design and optimal sizing of microgrids. In: Microgrids Design and Implementation. Springer; 2019. p. 337–67.
[9] Neto PBL, Saavedra OR, Oliveira DQ. The effect of complementarity between solar, wind and tidal energy in isolated hybrid microgrids. Renew Energy 2020;147:339–55.
[10] Chauhan A, Saini R. A review on integrated renewable energy system based power generation for stand-alone applications: Configurations, storage options, sizing methodologies and control. Renew Sustain Energy Rev 2014;38:99–120.
[11] Upadhyay S, Sharma M. A review on configurations, control and sizing methodologies of hybrid energy systems. Renew Sustain Energy Rev 2014;38:47–63.
[12] Lian J, Zhang Y, Ma C, Yang Y, Chaima E. A review on recent sizing methodologies of hybrid renewable energy systems. Energy Convers Manage 2019;199:112027.
[13] Khan MJ, Yadav AK, Mathew L. Techno economic feasibility analysis of different combinations of PV-wind-diesel-battery hybrid system for telecommunication applications in different cities of Punjab, India. Renew Sustain Energy Rev 2017;76:577–607.
[14] Akram U, Khalid M, Shafiq S. An improved optimal sizing methodology for future autonomous residential smart power systems. IEEE Access 2018;6:5986–6000.
[15] Malheiro A, Castro PM, Lima RM, Estanqueiro A. Integrated sizing and scheduling of wind/PV/diesel/battery isolated systems. Renew Energy 2015;83:646–57.
[16] Ngan MS, Tan CW. Assessment of economic viability for PV/wind/diesel hybrid energy system in southern peninsular Malaysia. Renew Sustain Energy Rev 2012;16:634–47.
[17] Mandal S, Das BK, Hoque N. Optimum sizing of a stand-alone hybrid energy system for rural electrification Bangladesh. J Cleaner Prod 2018;200:12–27.
[18] Altun AF, Kilic M. Design and performance evaluation based on economics and environmental impact of a PV-wind-diesel and battery standalone power system for various climates in Turkey. Renew Energy 2020;157:424–43.
[19] Dufo-López R, Bernal-Agustín JL, Yusta-Loyo JM, Domínguez-Navarro JA, Ramírez-Rosado IJ, Lujano J, et al. Multi-objective optimization minimizing cost and life cycle emissions of stand-alone PV-wind-diesel systems with batteries storage. Appl Energy 2011;88:4033–41.
[20] Bhuiyan FA, Yazdani A, Primak SL. Optimal sizing approach for islanded microgrids. IET Renew Power Gener 2015;9:166–75.
[21] Dufo-López R, Cristóbal-Monreal IR, Yusta JM. Optimisation of PV-wind-diesel-battery stand-alone systems to minimise cost and maximise human development index and job creation. Renew Energy 2016;94:280–93.
[22] Bilal BO, Sambou V, Kébé C, Ndiaye P, Ndongo M. Methodology to size an optimal stand-alone PV/wind/diesel/battery system minimizing the levelized cost of energy and the CO2 emissions. Energy Procedia 2012;14:1636–47.
[23] Bilal BO, Sambou V, Ndiaye P, Kébé C, Ndongo M. Study of the influence of load profile variation on the optimal sizing of a standalone hybrid PV/wind/battery/diesel system. Energy Procedia 2013;36:1265–75.
[24] Malheiro A, Castro PM, Lima RM, Estanqueiro A. Integrated sizing and scheduling of wind/PV/diesel/battery isolated systems. Renew Energy 2015;83:646–57.
[25] Ogunjuyigbe A, Ayodele T, Akinola O. Optimal allocation and sizing of PV/wind/split-diesel/battery hybrid energy system for minimizing life cycle cost, carbon emission and dump energy of remote residential building. Appl Energy 2016;171:153–71.
[26] Baneshi M, Hadianfard F. Techno-economic feasibility of hybrid diesel/PV/wind/battery electricity generation systems for non-residential large electricity consumers under southern Iran climate conditions. Energy Convers Manage 2016;127:233–44.
[27] Hossain M, Mekhilef S, Olatomiwa L. Performance evaluation of a stand-alone PV-wind-diesel-battery hybrid system feasible for a large resort center in South China Sea, Malaysia. Sustain Cities Soc 2017;28:358–66.
[28] Salisu S, Mustafa MW, Olatomiwa L, Mohammed OO. Assessment of technical and economic feasibility for a hybrid PV-wind-diesel-battery energy system in a remote community of north central Nigeria. Alexandria Eng J 2019;58:1103–18.

[29] Yang D, Jiang C, Cai G, Huang N. Optimal sizing of a wind/solar/battery/diesel hybrid microgrid based on typical scenarios considering meteorological variability. IET Renew Power Gener 2019;13:1446–55.
[30] Zhang L, Barakat G, Yassine A. Design and optimal sizing of hybrid PV/wind/diesel system with battery storage by using DIRECT search algorithm. In: 2012 15th International Power Electronics and Motion Control Conference (EPE/PEMC); 2012. p. DS3b.19-1–DS3b.19-7.
[31] Paliwal P, Patidar N, Nema R. Determination of reliability constrained optimal resource mix for an autonomous hybrid power system using particle swarm optimization. Renew Energy 2014;63:194–204.
[32] Borhanazad H, Mekhilef S, Ganapathy VG, Modiri-Delshad M, Mirtaheri A. Optimization of micro-grid system using MOPSO. Renew Energy 2014;71:295–306.
[33] Bukar AL, Tan CW, Lau KY. Optimal sizing of an autonomous photovoltaic/wind/battery/diesel generator microgrid using grasshopper optimization algorithm. Sol Energy 2019;188:685–96.
[34] Hatata A, Osman G, Aladl M. An optimization method for sizing a solar/wind/battery hybrid power system based on the artificial immune system. Sustain Energy Technol Assessm 2018;27:83–93.
[35] Fathy A, Kaaniche K, Alanazi TM. Recent approach based social spider optimizer for optimal sizing of hybrid PV/wind/battery/diesel integrated microgrid in aljouf region. IEEE Access 2020;8:57630–45.
[36] Ashraf MA, Liu Z, Alizadeh A, Nojavan S, Jermsittiparsert K, Zhang D. Designing an optimized configuration for a hybrid PV/diesel/battery energy system based on metaheuristics: A case study on gobi desert. J Cleaner Prod 2020;122467.
[37] Maleki A, Pourfayaz F. Sizing of stand-alone photovoltaic/wind/diesel system with battery and fuel cell storage devices by harmony search algorithm. J Energy Storage 2015;2:30–42.
[38] Li P, Li R, Cao Y, Li D, Xie G. Multiobjective sizing optimization for island microgrids using a triangular aggregation model and the levy-harmony algorithm. IEEE Trans Industr Inf 2018;14:3495–505.
[39] Diab AAZ, Sultan HM, Mohamed IS, Kuznetsov ON, Do TD. Application of different optimization algorithms for optimal sizing of PV/wind/diesel/battery storage stand-alone hybrid microgrid. IEEE Access 2019;7:119223–45.
[40] Bidram A, Davoudi A. Hierarchical structure of microgrids control system. IEEE Trans Smart Grid 2012;3:1963–76.
[41] Guerrero JM, Vasquez JC, Matas J, De Vicuña LG, Castilla M. Hierarchical control of droop-controlled AC and DC microgrids - A general approach toward standardization. IEEE Trans Ind Electron 2010;58:158–72.
[42] Vergara PP, López JC, Rey JM, da Silva LC, Rider MJ. Energy management in microgrids. In: Microgrids Design and Implementation. Springer; 2019. p. 195–216.
[43] Rey JM, Torres-Martínez J, Castilla M. Secondary control for islanded microgrids. In: Microgrids Design and Implementation. Springer; 2019. p. 171–93.
[44] Han Y, Li H, Shen P, Coelho EAA, Guerrero JM. Review of active and reactive power sharing strategies in hierarchical controlled microgrids. IEEE Trans Power Electron 2017;32:2427–51.
[45] Han Y, Li H, Shen P, Coelho EAA, Guerrero JM. Review of active and reactive power sharing strategies in hierarchical controlled microgrids. IEEE Trans Power Electron 2016;32:2427–51.
[46] de Souza Ribeiro LA, Saavedra OR, de Lima SL, de Matos J. Isolated micro-grids with renewable hybrid generation: The case of lençóis island. IEEE Trans Sustain Energy 2011;2:1–11.
[47] Foroutan VB, Moradi MH, Abedini M. Optimal operation of autonomous microgrid including wind turbines. Renew Energy 2016;99:315–24.
[48] Abdelaziz MMA, Farag HE, El-Saadany EF. Optimum reconfiguration of droop-controlled islanded microgrids. IEEE Trans Power Syst 2015;31:2144–53.
[49] Gupta Y, Doolla S, Chatterjee K, Pal BC. Optimal DG allocation and volt–var dispatch for a droop-based microgrid. IEEE Trans Smart Grid 2020;12:169–81.
[50] Y. Gupta, R. Nellikkath, K. Chatterjee, S. Doolla, Volt—var optimization and reconfiguration–reducing power losses in a droop based microgrid, in: 2020 IEEE International Conference on Power Electronics, Smart Grid and Renewable Energy (PESGRE2020), IEEE, 2020b, pp. 1–6.
[51] Roy NB, Das D. Optimal allocation of active and reactive power of dispatchable distributed generators in a droop controlled islanded microgrid considering renewable generation and load demand uncertainties. Sustain Energy Grids Netw 2021:100482.
[52] Subramanian L, Debusschere V, Gooi HB. Design and control of storage systems for voltage source controlled autonomous microgrids. In: 2019 IEEE Power & Energy Society General Meeting (PESGM). IEEE; 2019. p. 1–5.
[53] Sitompul S, Fujita G. Impact of advanced load-frequency control on optimal size of battery energy storage in islanded microgrid system. Energies 2021;14:2213.
[54] Mukhopadhyay B, Das D. Optimal multi-objective expansion planning of a droop-regulated islanded microgrid. Energy 2021;218:119415.
[55] Chen SX, Gooi HB, Wang MQ. Sizing of energy storage for microgrids. IEEE Trans Smart Grid 2012;3:142–51.
[56] Atia R, Yamada N. Sizing and analysis of renewable energy and battery systems in residential microgrids. IEEE Trans Smart Grid 2016;7:1204–13.
[57] Akram U, Khalid M, Shafiq S. Optimal sizing of a wind/solar/battery hybrid grid-connected microgrid system. IET Renew Power Gener 2018;12:72–80.
[58] Kaabeche A, Ibtiouen R. Techno-economic optimization of hybrid photovoltaic/wind/diesel/battery generation in a stand-alone power system. Sol Energy 2014;103:171–82.
[59] Ramli MA, Bouchekara H, Alghamdi AS. Optimal sizing of PV/wind/diesel hybrid microgrid system using multi-objective self-adaptive differential evolution algorithm. Renew Energy 2018;121:400–11.
[60] Borhanazad H, Mekhilef S, Ganapathy VG, Modiri-Delshad M, Mirtaheri A. Optimization of micro-grid system using MOPSO. Renew Energy 2014;71:295–306.
[61] Zhang Y, Wang J, Berizzi A, Cao X. Life cycle planning of battery energy storage system in off-grid wind-solar-diesel microgrid. IET Gener Transmiss Distrib 2018;12:4451–61.
[62] Vergara PP, López JC, da Silva LCP, Rider MJ. Economic impact of the active power droop gain in droop-based islanded microgrids. In: 2019 IEEE Milan PowerTech; 2019. p. 1–6.
[63] Lujano-Rojas JM, Monteiro C, Dufo-López R, Bernal-Agustín JL. Optimum load management strategy for wind/diesel/battery hybrid power systems. Renew Energy 2012;44:288–95.
[64] Shi W, Li N, Chu C, Gadh R. Real-time energy management in microgrids. IEEE Trans Smart Grid 2017;8:228–38.
[65] Vergara PP, Rey JM, da Silva LCP, Ordóñez G. Comparative analysis of design criteria for hybrid photovoltaic/wind/battery systems. IET Renew Power Gener 2017;11:253–61.
[66] Sun Y, Hou X, Yang J, Han H, Su M, Guerrero JM. New perspectives on droop control in AC microgrid. IEEE Trans Industr Electron 2017;64:5741–5.
[67] Guerrero JM, de Vicuna LG, Matas J, Castilla M, Miret J. A wireless controller to enhance dynamic performance of parallel inverters in distributed generation systems. IEEE Trans Power Electron 2004;19:1205–13.
[68] Yu K, Ai Q, Wang S, Ni J, Lv T. Analysis and optimization of droop controller for microgrid system based on small-signal dynamic model. IEEE Trans Smart Grid 2016;7:695–705.